Conversion of Methanol to Gasoline: A New Mechanism for Formation of the First Carbon–Carbon Bond

James E. Jackson*,[1a-c] and Frederick M. Bertsch[1b,d]

Contribution from the Department of Chemistry and Center for Fundamental Materials Research, Michigan State University, East Lansing, Michigan 48824, and East Lansing High School, 509 Burcham Road, East Lansing, Michigan 48823. *Received April 25, 1990*

Abstract: A general mechanism is proposed for the critical first C–C bond forming event in the H-ZSM-5-zeolite-catalyzed and related methanol to gasoline (MTG) conversion reactions. We begin with the assumption that the Pearson reaction, in which methanol is converted to hydrocarbons at 200 °C by polyphosphoric acid (PPA), operates by a mechanism similar to the zeolite-catalyzed processes. Results from the literature are combined with new experimental and computational work to present a simple, thermochemically reasonable picture of the overall transformation cycle. Consistent with established gas-phase thermochemistry and recent solid-state NMR results, carbon monoxide appears to be the operative catalytic species. According to the new scheme, after its slow initial generation (induction period), CO is methylated, producing an acylium ion, which is then deprotonated; subsequent methylation of the resulting ketene represents the key new C–C bond forming step. Loss of ethylene completes the cycle. Ab initio calculations support the kinetic and thermodynamic accessibility of the overall reaction sequence. Solution NMR experiments on the Pearson reaction show no exchange of protons between the acidic *H*O and the hydridic *H*CH_2OX protons of methanol or its phosphate esters, even under conditions where substantial hydrocarbon is being generated. This result, along with simple thermochemical arguments, renders highly doubtful the widely invoked pathway via methylation of an oxonium methylide.

Introduction

This paper points out a unifying and energetically plausible mechanism for industrial and laboratory methanol to gasoline (MTG) processes.[2] The new pathway is consistent with all available data and involves no bizarre intermediates. Moreover, it posits no unique catalyst properties beyond strong Brönsted acidity, and each step has reasonable precedents. The operative catalyst is carbon monoxide, whose presence has several times been noted in MTG processes.[3,4]

The most familiar MTG conversion is the "Mobil Process",[5] in which H-ZSM-5, a high-silica aluminosilicate zeolite, catalyzes the dehydration of methanol or dimethyl ether into hydrocarbons, typically at 300–400 °C. Other oxides such as WO_3/Al_2O_3 have also been shown to induce this reaction, albeit with poor efficiencies and excess methane production.[6] Less widely known is the Pearson reaction, in which polyphosphoric acid (PPA) effects the MTG transformation at 200 °C.[7] The Pearson reaction is unique in its relative mildness. We are not aware of any other oxide-catalyzed reaction that forms new C–C bonds between commonplace C_1 fragments at such low temperatures.

The economic significance of MTG technology is enormous. It has therefore engendered widespread attempts to understand and control these reactions. The shape selectivity of zeolite catalysts has drawn considerable attention,[8a-d] but an even more fundamental question concerns the initial C–C bond forming step(s) whereby methanol (CH_3OH), a C_1 compound, is transformed into a C_2 species such as ethylene. As raw petroleum resources diminish, the net transformation will become more valuable, especially if methanol's price continues to drop with its development as an alternative automotive fuel.[8e] Naturally, a thorough molecular level understanding could ultimately contribute to the design of catalysts with improved efficiency and specificity.

The molecular mechanism for MTG chemistry over simple acidic oxide catalysts is still in debate, in spite of a great deal of investigation and speculation. Proposals for the mechanism have been put forward by Derouane,[9] Olah,[10] Chang,[11] Hutchings,[12]

Scheme I. Oxonium Ylide Mechanism

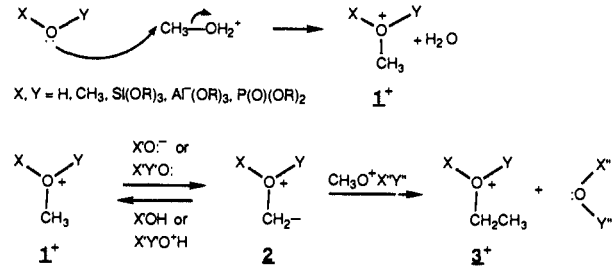

Scheme II. Trimethyloxonium Tetrafluoroborate Experiment

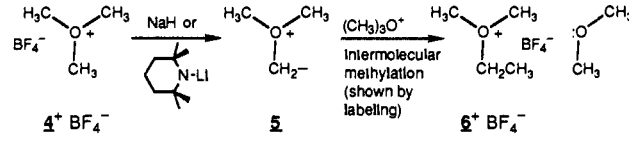

(1) (a) Camille and Henry Dreyfus Distinguished Young Faculty. (b) Michigan State University. (c) Center for Fundamental Materials Research. (d) East Lansing High School.

(2) (a) Chang, C. D. *Hydrocarbons from Methanol*; Dekker: New York, 1983. (b) Olah, G. A.; Doggweiler, H.; Felberg, J. D.; Frohlich, S.; Grdina, M. J.; Karpeles, R.; Keumi, T.; Inaba, S.-i.; Ip, W. M.; Lammertsma, K.; Salem, G.; Tabor, D. C. *J. Am. Chem. Soc.* **1984**, *106*, 2143. (c) Chang, C. D. *Perspectives in Molecular Sieve Science*; Flank, W. H., Whyte, T. E., Jr., Eds.; ACS Symposium Series 368; American Chemical Society: Washington, DC, 1988; Chapter 39.

(3) (a) Anderson, M. W.; Klinowksi, J. *J. Am. Chem. Soc.* **1990**, *112*, 10. (b) Anderson, M. W.; Klinowski, J. *Nature* **1989**, *339*, 200. (c) Dwyer, J. *Nature* **1989**, *339*, 174.

(4) (a) Chu, C. T. W.; Chang, C. D. *J. Catal.* **1984**, *86*, 297. (b) Chang, C. D.; Chu, C. T. W.; Socha, R. F. *J. Catal.* **1984**, *86*, 289. (c) Kaeding, W. W.; Butter, S. A. *J. Catal.* **1980**, *61*, 155.

(5) (a) Chang, C. D.; Silvestri, A. J. *J. Catal.* **1977**, *47*, 249. (b) Wiesz, P. B. CHEMTECH **1973**, *3*, 498. (c) Meisel, S. L.; McCullough, J. P.; Lechtaler, C. H.; Weisz, P. B. CHEMTECH **1976**, *6*, 86.

(6) (a) Hunter, R.; Hutchings, G. J. *J. Chem. Soc., Chem. Commun.* **1987**, 377. (b) Hutchings, G. J.; Jansen van Rensburg, L.; Pickl, W.; Hunter, R. *J. Chem. Soc., Faraday Trans. 1* **1988**, *84*, 1311. See also ref 2b.

(7) (a) Pearson, D. E. *J. Chem. Soc., Chem. Commun.* **1974**, 397. (b) Pearson, D. E. *Chem. Eng. News* **1983**, Feb 14, p 50. (c) Pearson, D. E. Personal communication to J. E. Jackson, May 1989.

(8) (a) See, for example: (a) Csiscevy, S. M. *Zeolites* **1984**, *4*, 202. (b) Chen, N. Y.; Garwood, W. E. *Catal. Rev. Sci. Eng.* **1986**, *28*, 185. (c) Derouane, E. G.; Vanderdeken, D. *Appl. Catal.* **1988**, *45*, 15. (d) Fraenkel, D.; Levy, M. *J. Catal.* **1989**, *119*, 108. (e) CH_3OH as Fuel of the Future. *Consumer Reports* **1990**, Jan, 11.

(9) (a) Derouane, E. G.; Nagy, J. B.; Dejaifva, P.; van Hooff, J. H. C.; Spekman, B. P.; Védrine, J. C.; Naccache, C. *J. Catal.* **1978**, *53*, 40. (b) Nagy, J. B.; Gilson, J. P.; Derouane, E. G. *J. Mol. Catal.* **1979**, *5*, 393.

(10) (a) Olah, G. A.; Doggweiler, H.; Felberg, J. D. *J. Org. Chem.* **1984**, *49*, 2112, 2116. (b) Olah, G. A.; Prakash, G. K. S.; Ellis, R. W.; Olah, J. A. *J. Chem. Soc., Chem. Commun.* **1986**, 9. (c) Olah, G. A. *Pure Appl. Chem.* **1981**, *53*, 201. See also ref 2b.

(11) Chang, C. D.; Hellring, S. D.; Pearson, J. A. *J. Catal.* **1989**, *115*, 282. See also refs 2a,c.

0002-7863/90/1512-9085$02.50/0

Scheme III. CO-Catalyzed Ethene and Propene Formation from Methanol

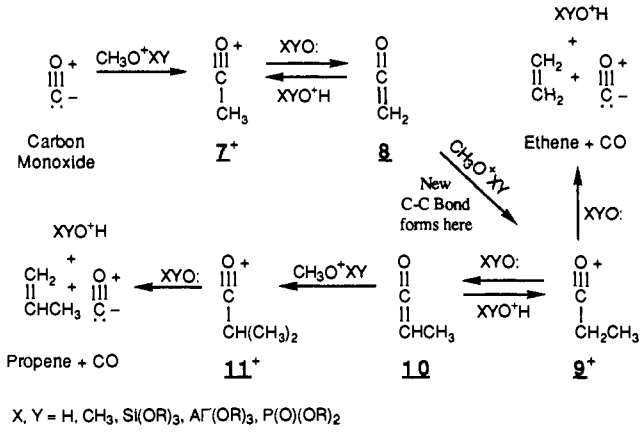

Mole,[13] and others,[14] but there is little definitive evidence to distinguish among them. Most of the postulated pathways represent unprecedented reactions, so it is of fundamental interest to determine how they might occur.

Currently, the most popular mechanism for MTG processes involves methylation of an oxonium ylide (Scheme I). Olah[10] and others[14] have suggested that a methyloxonium species $\mathbf{1}^+$ might be deprotonated to make methyleneoxonium ylide **2**, which would then be rapidly methylated by a second methyloxonium equivalent, yielding ethyloxonium ion $\mathbf{3}^+$. Recent solid-state NMR[15] and IR[16] work, most notably from the group of Haw,[15a-e] has probed the role of zeolite-bound alkyl groups in MTG chemistry and in olefin oligomerization, cracking, and dehydration reactions. These studies have clearly differentiated between surface-bound and more mobile species (alcohols, ethers, and olefins) and have established the presence and high reactivity of the bound oxonium species made by alkylation of zeolite surface oxygens.

In model studies with $(CH_3)_3O^+BF_4^-$ ($4^+BF_4^-$), Olah et al.[10a] and Rimmelin et al.[14a,b] found that the strong bases NaH and lithium tetramethylpiperidide can accomplish the required deprotonation (Scheme II), yielding methylenedimethyloxonium ylides **5**. Methylation of **5** then makes ethyldimethyloxonium ion $\mathbf{6}^+$, which ultimately decomposes to give the ethylene observed. It seems unlikely that sites as strongly basic as the above bases could coexist with the acid sites in a thoroughly H^+-exchanged zeolite, to say nothing of fluid polyphosphoric acid solution. Furthermore, experimental and theoretical evidence (vide infra) suggests that formation of methylides by deprotonation of methyloxonium salts is in general a difficult process, especially if opportunities for competing methyl transfer are available. In Olah's studies of trimethyloxonium deprotonation with NaH as the base, considerable methane was produced;[10a] thus, NaH—normally strongly basic and a poor donor of nucleophilic hydride—was substantially diverted from deprotonation by the highly electrophilic but weakly acidic trimethyloxonium ion.

In this work, we propose a new mechanism in which carbon monoxide is the effective catalyst for the first C–C bond formation in MTG conversion. CO is already established as the first-formed species in reaction of methanol over H-ZSM-5 zeolites;[3] we now outline an active role for this simple molecule. It is the entity that activates methyl groups, originally from CH_3OH, to function as carbon nucleophiles in the form of ketenes. Scheme III displays the proposed reaction scheme, a CO-catalyzed sequence in which each step is thermodynamically reasonable and no unusual structures or special stabilization of high-energy intermediates need to be invoked.

Methods

NMR Studies. The PPA–methanol system is a homogeneous, if viscous, liquid, which includes three NMR-active nuclei: ^1H, ^{13}C, and ^{31}P. Viscosity problems are overcome by gentle heating (60–100 °C) of the samples in the NMR probe. A fourth nucleus, ^2H, is readily and specifically introduced in the form of selectively deuterated methanol. Hydrogen exchange between OH and CH sites may then be tracked, as may the origins of the protons in the hydrocarbon products. The couplings observed between ^1H or ^{13}C and ^{31}P yield information about P–O–C–H connectivity in alkyl phosphates. Furthermore, by using appropriate references, we are able to search specifically for species such as C_2 and higher phosphate esters.

The solutions' viscosity may also be turned to advantage. When the sealed NMR sample tubes are inverted at room temperature, the solutions do not flow. Thus, in addition to the solution experiments described above, we use NMR directly to probe the gaseous reaction products in the headspace. This approach is much less sensitive to trace gases than conventional methods of gas analysis, such as coupled gas chromatography–mass spectrometry (GC–MS). However, it is perfectly satisfactory in this nontrace application, and since it is noninvasive, we are able to examine the same reacting system from beginning to end, avoiding uncertainties that come from comparing different preparations of a given reaction mixture.

In a typical experiment, a mixture of methanol and P_2O_5, methanol and PPA, or trimethyl phosphate and PPA was placed in a thick-walled NMR tube, degassed by three freeze–pump–thaw cycles, and sealed under vacuum. ^1H, ^{13}C, ^{31}P, and when appropriate, ^2H NMR spectra were obtained for the solution by gently warming it to lower its viscosity, narrowing the observed peaks. Inverting the unheated tube without spinning permitted spectra of the gases in the headspace to be obtained. Thus far, we have only been practically able to observe ^1H spectra in the gas phase, but with the use of ^{13}C-labeled starting materials, it will also become possible to use this nucleus as a gas-phase probe.

Ab Initio Calculations. Computational studies were performed with the GAUSSIAN86 suite of programs[17] running on a Digital Equipment VAXstation 3200 computer. Fully optimized structures for the listed neutral, protonated, methylated, and methylenated species were computed with 3-21G, 6-31G*, and 6-31+G* basis sets.[18] Total energies were then calculated at the MP3/6-31+G* level,[19] and zero-point and thermal corrections were made with vibrational frequencies obtained by diagonalizing the Hessian force constant matrix at the 3-21G level.[20] The vibrational analysis served to characterize minima and transition structures optimized under symmetry constraints; these had, respectively, 0 or 1 negative eigenvalue of the Hessian matrix as appropriate. From the calculated energies of the structures above, values were extracted for the proton, methyl cation, and methylene affinities of the relevant species for comparison with available experimental numbers.[21a] In some cases,

(12) Hutchings, G. J.; Gottschalk, F.; Hall, M. V. M.; Hunter, R. *J. Chem. Soc., Faraday Trans. 1*, **1987**, *83*, 571. See also ref 6.

(13) (a) Mole, T. *J. Catal.* **1983**, *84*, 423. (b) Mole, T.; Bell, G.; Sedden, G. *J. Catal.* **1983**, *84*, 435. (c) Mole, T., Whiteside, J. A. *J. Catal.* **1982**, *75*, 284.

(14) (a) Rimmelin, P., Taghavi, H., Sommer, J. *J. Chem. Soc., Chem. Commun.* **1984**, 1210. (b) Rimmelin, P., Brenner, A., Fischer, K., Sommer, J. *J. Chem. Soc., Chem. Commun.* **1986**, 1498. (c) Van den Berg, J. P.; Wolthuizen, J. P.; van Hooff, J. H. C. In *Proceedings, 5th International Conference on Zeolites*; Rees, L. V. C., Ed.; Heyden: London, England, 1980; p 649. (d) Lee, C. S.; Wu, M. M. *J. Chem. Soc., Chem., Commun.* **1985**, 250.

(15) (a) Lazo, N. D.; Munson, E. J.; White, J. L.; Haw, J. F. *J. Am. Chem. Soc.*, in press. (b) Haw, J. F. Personal communication, July 1990. We thank Professor Haw for sharing these results prior to publication. (c) Zardkoohi, M.; Haw, J. F.; Lunsford, J. H. *J. Am. Chem. Soc.* **1987**, *109*, 5278. (d) Haw, J. F.; Richardson, B. R.; Oshiro, I. S.; Lazo, N. D.; Speed, J. A. *J. Am. Chem. Soc.* **1989**, *111*, 2052. (e) Richardson, B. R.; Lazo, N. D.; Schettler, P. D.; White, J. L.; Haw, J. F. *J. Am. Chem. Soc.* **1990**, *112*, 2886. (f) Anderson, M. W.; Klinowski, J. *J. Chem. Soc., Chem. Commun.* **1990**, 918. (g) Aronson, M. T.; Gorte, R. J.; Farneth, W. E.; White, D. *J. Am. Chem. Soc.* **1989**, *111*, 840.

(16) Forester, T. R.; Howe, R. F. *J. Am. Chem. Soc.* **1987**, *109*, 5076.

(17) Frisch, M. J.; Binkley, J. S.; Schlegel, H. B.; Ragavachari, K.; Melius, C. F.; Martin, R. L.; Stewart, J. J. P.; Bobrowicz, F. W.; Rohlfing, C. M.; Kahn, L. R.; Defrees, D. J.; Seeger, R.; Whiteside, R. A.; Fox, D. J.; Fleuder, E. M.; Pople, J. A. *Gaussian 86*; Carnegie-Mellon Quantum Chemistry Publishing Unit: Pittsburgh, PA, 1984; Revision C. We thank Professor J. F. Harrison of this department for making this program available to us.

(18) Basis sets. (a) 3-21G: Binkley, J. S., Pople, J. A.; Hehre, W. J. *J. Am. Chem. Soc.* **1980**, *102*, 939. (b) 6-31G*: Hariharan, P. C.; Pople, J. A. *Theor. Chim. Acta* **1973**, *28*, 213. (c) 6-31+G: Spitznagel, G. W.; Clark, T.; Chandrasekhar, J.; Schleyer, P. v. R. *J. Comput. Chem.* **1982**, *3*, 363.

(19) We employ the standard Gaussian series[17] abbreviation "MPn" meaning the *n*th order Møller–Plesset perturbational method for estimating electron correlation energy. See: (a) Møller, C.; Plesset, M. S. *Phys. Rev.* **1934**, *46*, 618. (b) Binkley, J. S.; Pople, J. A. *Int. J. Quantum Chem.* **1975**, *9*, 229. (c) Pople, J. A.; Binkley, J. S.; Seeger, R. *Int. J. Quantum Chem. Symp.* **1976**, *10*, 1.

(20) (a) Pople, J. A.; Krishnan, R.; Schegel, H. B.; Binkley, J. S. *Int. J. Quantum Chem. Symp.* **1979**, *13*, 225.

Table I.[a,b] Experimental Gas-Phase Energies of Proposed MTG Intermediates

X	$\Delta H_f(X)$	PA[b]	MCA	$\Delta H_f(XH^+)$
CH_2 ($^1A_1$ state)	102	206	148	261.3
CH_2CH_2	12.5	163	63	215.6
CH_2CHCH_3	4.8	180	83	190.9
$CH_2C(CH_3)_2$	-4.0	196	99	165.8
OC:	-26.4	142	78	197.3
$OCCH_2$ (**8**)	-11.4	198	109	156.0
$OCCHCH_3$ (**10**)	-25	199	103 (est)[c]	141
H_2O	-57.8	167	68	141.4
CH_3OH	-48.2	182	83	135.6
$CH_2{-}OH_2^+$	38.1[d]	268	178	135.6
$(CH_3)_2O$	-44.0	192	92 (est)[e]	130

[a] Abbreviations: PA = proton affinity; MCA = methyl cation affinity. All these values listed in kilocalories per mole. [b] All ΔH_f values refer to 298 K and were taken from ref 21a except where otherwise noted. The $\Delta H_f(H^+)$ is 365.7 kcal/mol (stationary electron convention). [c] The $\Delta H_f(i\text{-}PrCO^+)$ was estimated as follows: $PA(H_2CCMe_2)$ = 195.9; $PA(MeHCCMe_2)$ = 197.6; $PA(Me_2CCMe_2)$ = 199.1; PA-($H_2C{=}CO$) = 198; PA($MeHC{=}CO$) = 199.4 kcal/mol. Estimated $PA(Me_2C{=}CO)$ = ~201; $\Delta H_f(Me_2CCO)$ = -32; therefore, $\Delta H_f(i\text{-}PrCO^+)$ ~ 133. This allows the estimation of the MCA($MeHC{=}CO$). [d] Taken from relative energies of CH_3OH and $CH_2{-}OH_2^+$ calculated by Pople et al. (see ref 31). [e] Estimated from the approximate relationship MCA(ROR') = PA(ROR') + 100 kcal/mol. (See ref 21b.)

established methyl cation affinity/proton affinity (MCA/PA) relationships were used to estimate experimental MCA values.[21b]

Results

NMR Studies. With the NMR techniques outlined previously, we have made several observations that limit the possible mechanisms of hydrocarbon formation. Methanol combines at room temperature with P_2O_5 or PPA to form mixtures of methyl phosphate and polyphosphate esters. The methyl protons are strongly coupled to the phosphate's ^{31}P nuclei in such esters. By starting with a mixture of $(CH_3O)_3PO$ in PPA and observing changes in the ^{31}P spectra, we have shown that equilibration among the methyl phosphate esters is a facile process at 100 °C, well before any hydrocarbons are seen. A labeling experiment in which CD_3OD was substituted for methanol showed no incorporation of ^1H from PPA into deuterated methyl groups attached to oxygen. Under conditions that generated substantial quantities of (^1H-containing) hydrocarbon products, no ^1H was observed in the well-separated region (~3.5 ppm) of the proton spectrum where CH_3OX resonates.[3] Thus, protons from the acidic OH population apparently do not exchange with those in the CH sites, even under conditions where hydrocarbons are being produced. The fact that some ^1H appears in the hydrocarbon products is unsurprising in light of the likely intermediacy of olefinic species such as ethylene that may easily exchange protons in acids. Although the hydrocarbon products unmistakably show paraffinic CH_2 resonances around -1 to +2.5 ppm, we do not detect ethoxy groups, whose OCH_2 fragments can be easily resolved. Under our reaction conditions (200 °C, 0-10 h), the only aromatic species we find is a tiny trace of benzene that arises at long reaction times (>2 h). Consistent with Pearson's early observations, we have found that at high conversions a clear organic layer separates from the yellow PPA-methanol mixture. Using differences in the fluidity of the layers, we can easily take separate spectra for each, which allows us to independently characterize the two liquid phases.

Headspace ^1H NMR has shown two principal gas-phase species:[22] dimethyl ether and ethylene. Dimethyl ether, the simple dehydration product of methanol, vastly outweighs the ethylene. Although Pearson found that methane was produced in similar reactions,[7] we have not observed gas-phase resonances assignable to it, in spite of the well-separated position of the protons in methane from any possible interfering resonances. Similarly, hydrogen, if present, is also below observable levels. Because of a combination of low concentration and long relaxation times, the corresponding gas-phase carbon spectra have not yet been obtainable. It is clear that gas-phase ^{13}C studies will require isotopically enriched starting materials.

Table II. Experimental Gas-Phase Cation Affinities of CO, N_2, and H_2O

cation		CO	N_2	H_2O	comments
proton	PA	142	118.2	166.5	$\Delta H_f(H_3O^+)$ = 141
methyl	MCA	78	45.3	67.5	$\Delta H_f(MeOH_2^+)$ = 136
ethyl	ECA	48		37	$\Delta H_f(EtOH_2^+)$ = 121
isopropyl	PCA	31 (est)[b]		24	$\Delta H_f(i\text{-}PrOH_2^+)$ = 109
tert-butyl	BCA			11	$\Delta H_f(t\text{-}BuOH_2^+)$ = 97

[a] See notes *a* and *b*, Table I. ECA = ethyl cation affinity, PCA = isopropyl cation affinity, BCA = *tert*-butyl cation affinity. [b] From estimated $\Delta H_f(i\text{-}PrCO^+)$; see note *c*, Table I.

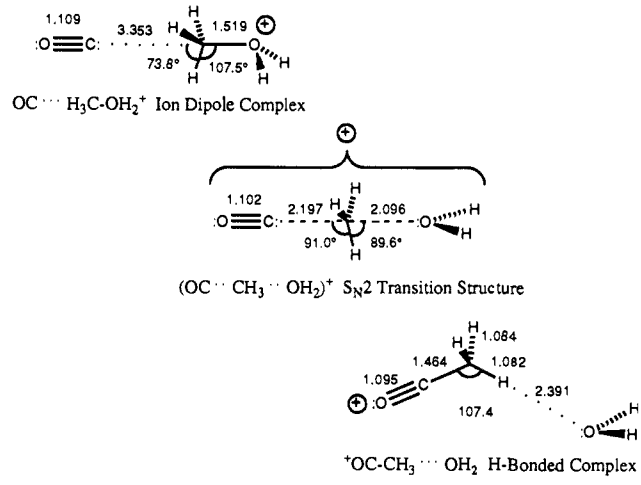

Figure 1. Partial geometries (distances in angstroms, angles in degrees) of ion-dipole complexes and the transition structure for S_N2 displacement of H_2O from $CH_3OH_2^+$ by CO. All these structures were calculated within C_s symmetry at the RHF level with the three basis sets. The selected geometrical variables shown here were computed at the 6-31+G* level.

Computational Studies. Tables I and II present relevant experimental gas-phase data for the proton and alkyl cation transfer reactions in Schemes II and III.[21] Table III lists the total energy, PA, and MCA results for the species of Scheme III computed at five different ab initio levels, and Table IV displays the analogous numbers for the oxonium ylide pathway of Scheme I. As in Olah's studies,[11] the hypothetical methyloxonium ion intermediates of Scheme I are modeled as trimethyloxonium ions; we also report the analogous calculations for protonated methanol. A huge amount of high-level theoretical work on proton affinities has been reported, including many of the molecules discussed herein; these efforts have been recently reviewed.[21c,d] We have opted to compute our own less rigorous but internally consistent data set using the 6-31+G* basis, which was chosen in order to properly represent the carbanionic centers in oxonium ylides. Within this basis, computations on transition structures and other points along the reaction paths of interest are still affordable on our VAX and, for the level of accuracy required here, are quite satisfactory.

In addition to examining minima along the reaction path, we have calculated the two ion-molecule complexes and the S_N2

(21) (a) Lias, S. G.; Bartmess, J. E.; Liebman, J. F.; Holmes, J. L.; Levin, R. D.; Mallard, W. G. Gas Phase Ion and Neutral Thermochemistry. *J. Phys. Chem. Ref. Data* **1988**, *17*, Supplement 1. (b) McMahon, T. B.; Heinis, T.; Nicol, G.; Hovey, J. K.; Kebarle, P. *J. Am. Chem. Soc.* **1988**, *110*, 7591. (c) Dixon, D. A.; Lias, S. G. In *Molecular Structure and Energetics*; Liebman, J. F., Greenberg, A., Eds.; VCH Publishers: New York, 1987; Vol. 2, Chapter 7. (d) Del Bene, J. E. In *Molecular Structure and Energetics*; Liebman, J. F., Greenberg, A., Eds.; VCH Publishers: New York, 1986; Vol. 1, Chapter 9.

(22) Gas-phase chemical shifts were measured relative to external $Si(CH_3)_4$ vapor and were in agreement with literature values; see: Petrakis, L., Sederholm, C. H. *J. Chem. Phys.* **1961**, *35*, 1174.

Table III. Theoretical Energies: Methylated CO Series[a]

level	3-21G	6-31G*	6-31+G*	MP2	MP3
H^+	(0.0)	(0.0)	(0.0)	(0.0)	(0.0)
CH_2 ($^1A_1$ state)	-38.651 85	-38.872 37	-38.876 55	-38.975 54	-38.993 24
		VIB = 0.020 35; PA = 209.1 (206)			
CH_3^+	-39.009 13	-39.230 64	-39.230 89	-39.325 55	-39.342 04
		VIB = 0.035 99			
CH_2CH_2	-77.600 99	-78.031 72	-78.035 82	-78.290 50	-78.311 13
		VIB = 0.058 04; PA = 156.2 (163)			
$CH_3CH_2^+$	-77.872 61	-78.311 23	-78.311 50	-78.544 17	-78.569 87
		VIB = 0.067 83			
OC:	-112.093 30	-112.737 88	-112.742 14	-113.025 86	-113.024 17
		VIB = 0.007 64; PA = 134.3 (142); MCA = 67.8 (78)			
OCH^+	-112.321 13	-112.965 92	-112.966 76	-113.255 69	-113.251 16
		VIB = 0.020 59			
$OCCH_2$ (**8**)	-150.876 53	-151.724 67	-151.729 89	-152.154 19	-152.158 97
		VIB = 0.038 02; PA = 194.3 (198); MCA = 97.9 (109)			
OC^+CH_3 (7^+)	-151.201 31	-152.059 30	-152.060 49	-152.475 88	-152.482 21
		VIB = 0.051 65			
$OCCHCH_3$ (**10**)	-189.694 88	-190.759 16	-190.764 13	-191.320 38	-191.334 25
		VIB = 0.070 48; PA = 199.7 (199)			
$OC^+CH_2CH_3$ (9^+)	-190.030 36	-191.102 99	-191.104 36	-191.649 99	-191.665 82
		VIB = 0.083 75			

[a] Total energies are listed in hartrees (H); 1 H = 627.5 kcal/mol. Geometries for all species were computed with RHF wave functions at each of the three basis sets listed. MP*n*/6-31+G* calculations were then run at the RHF/6-31+G* optimized geometries within the frozen-core approximation. Thus, the headings shown represent (in standard notation) RHF/3-21G//RHF/3-21G; RHF/6-31G*//RHF/6-31G*; RHF/6-31+G*//RHF/6-31+G*; MP2/6-31+G*//RHF/6-31+G*; and MP3/6-31+G*//RHF/6-31+G* total energies. Listed values represent calculations at the five computational levels, respectively. Experimental values for these quantities, where known, are shown in parentheses. VIB indicates energy correction due to zero-point and thermal energy (at 298 K), as calculated at the 3-21G level.

Table IV. Theoretical Energies: Methylated Water Series

level	3-21G*	6-31G*	6-31+G*	MP2	MP3
H_2O:	-75.585 96	-76.010 75	-76.017 74	-76.208 74	-76.213 03
		VIB = 0.024 61;[b] PA = 161.3 (166.5); MCA = 63.5 (67.5)			
H_3O^+	-75.891 23	-76.286 56	-76.290 60	-76.476 43	-76.483 58
		VIB = 0.038 06			
CH_3OH	-114.398 02	-115.035 42	-115.040 97	-115.356 47	-115.371 02
		VIB = 0.057 74; PA = 177.2 (181.5); MCA = 78.3 (83.1)			
$CH_2OH_2^+$	-114.270 09	-114.896 62	-114.905 74	-115.204 82	-115.224 68
		VIB = 0.053 44; PA = 266.3 (268); MCA = 173.0 (178)			
$CH_3O^+H_2$	-114.724 92	-115.338 99	-15.340 66	-115.648 58	-115.666 38
		VIB = 0.070 76			
$CH_3CH_2O^+H_2$	-153.556 28	-154.386 64	-154.388 68	-154.827 51	-154.855 12
		VIB = 0.102 09			
$(CH_3)_2O$:	-153.213 21	-154.064 75	-154.069 43	-154.513 08	-154.536 90
		VIB = 0.089 82; PA = 186.4 (192.1); MCA = 85.6 (92-3)[a]			
$(CH_3)_2O^+H$	-153.552 86	-154.382 38	-154.384 05	-154.818 67	-154.846 35
		VIB = 0.102 20			
$(CH_3)_2O^+CH_2$ (**5**)	-191.898 27	-192.949 49	-192.958 42	-193.523 62	-193.560 08
		VIB = 0.118 02; PA = 280.8			
$(CH_3)_2O^+CH_3$ (4^+)	-192.378 04	-193.421 48	-193.422 88	-193.988 63	-194.025 17
		VIB = 0.153 33			

[a] This MCA calculated from the PA and MCA–PA correlations; see Table II in ref 21b. [b] VIB = vibrational energy contribution at 298 K = zero-point energy + ΔH(0–298 K) as calculated at the 3-21G level.

transition state for the transfer of a methyl cation from H_2O to CO. Results from this reaction path calculation are summarized in Table V and Figure 1. Similar calculations for the methylation of ketene are summarized in Table VI and Figure 2. A graphic summary of the experimental and theoretically calculated reaction energy profiles for the CO-catalyzed process of Scheme III and the XYO:-catalyzed process of Scheme II is given in Figure 3. This illustration permits direct comparisons to be made on energetic terms between the two pathways.

The ab initio calculations provide common ground from which to evaluate the various potential intermediates along the candidate reaction paths. It must be borne in mind that these calculations simulate gas-phase behavior, completely ignoring effects due to the highly polar PPA–methanol or zeolite reaction medium.[23] It is possible that strongly polarized structures such as ylides might be preferentially stabilized in such environments, invalidating

(23) (a) We have computationally surveyed a wide range of methyloxonium ions and their corresponding oxonium methylides at semiempirical and ab initio levels of theory and find no evidence for special stabilization by the other ligands on oxygen (X, Y in Schemes I and II). For example, adding phosphate (protonated or not) or silyl groups does not significantly change the energetic costs of methyl deprotonation. (Berisch, F. Unpublished results.) (b) A combined molecular and quantum mechanical treatment has suggested that the highly polarized environment inside the ZSM-5 cage may significantly distort the methanol molecule; see: Vetrivel, R.; Catlow, C. R. A.; Colbourn, E. A. *J. Phys. Chem.* **1989**, *93*, 4594.

Table V. Theoretical Energies for the S_N2 Reaction $CO + CH_3OH_2^+ \rightarrow CH_3CO^+ + H_2O$[a]

level	3-21G	6-31G*	6-31+G*	MP2	MP3
$CO + CH_3OH_2^+$ separated species	−226.818 22	−228.076 87	−228.082 80	−228.674 44	−228.690 55
	VIB = 0.078 40; E_{rel} = [0.0]				
$OC\cdots CH_3OH_2^+$ ion-dipole complex	−226.823 27	−228.080 49	−228.085 73	−228.680 04	−228.695 35
	VIB = 0.081 00; E_{rel} = −1.4				
$(OC\cdots CH_3\cdots OH_2)^+$ S_N2 TS	−226.794 74	−228.054 97	−228.060 52	−228.653 21	−228.666 99
	VIB = 0.078 80; E_{rel} = 15.0				
$OCCH_3^+\cdots OH_2$ ion-dipole complex	−226.825 15	−228.098 28	−228.104 26	−228.713 19	−228.723 55
	VIB = 0.079 62; E_{rel} = −19.6				
$OCCH_3^+ + H_2O$ separated species	−226.787 27	−228.070 05	−228.078 23	−228.684 62	−228.695 24
	VIB = 0.076 26; E_{rel} = −4.3 (−10)				

[a] See Table I, note *a*. Listed values represent calculations at the five computational levels, respectively. Experimental values for these quantities, where known, are shown in parentheses.

Table VI. Theoretical Energies for the S_N2 Reaction $OCCH_2 + H_3COH_2^+ \rightarrow {}^+OCCH32CH_3 + H_2O$[a]

level	3-21G	6-31G*	6-31+G*	MP2	MP3
$OCCH_2 + CH_3OH_2^+$ separated species	−265.601 45	−267.063 66	−267.070 55	−267.802 77	−267.825 35
	VIB = 0.108 78; E_{rel} = [0.0]				
$OCCH_2\cdots CH_3OH_2^+$ ion-dipole complex	−265.620 09	−267.076 63	−267.083 15	−267.815 85	
	VIB = 0.110 78; E_{rel} = −7.0				
$(OCCH_2\cdot CH_3\cdot OH_2)^+$ S_N2 TS	−265.591 41	−267.056 17	−267.061 44	−267.799 77	
	VIB = 0.109 51; E_{rel} = +2.3				
$OCCH_2CH_3^+\cdots OH_2$ ion-dipole complex	−265.650 30				
	VIB = 0; E_{rel} = −30.7 (No vib)				
$OCCH_2CH_3^+ + H_2O$ separated species	−265.616 32	−267.113 74	−267.122 10	−267.858 73	−267.878 85
	VIB = 0.108 36; E_{rel} = −33.8 (−41)				

[a] See Table I, note *a*. Listed values represent calculations at the five computational levels, respectively. Experimental values for these quantities, where known, are shown in parentheses. All E_{rel} values correspond to the highest available calculational level for that species.

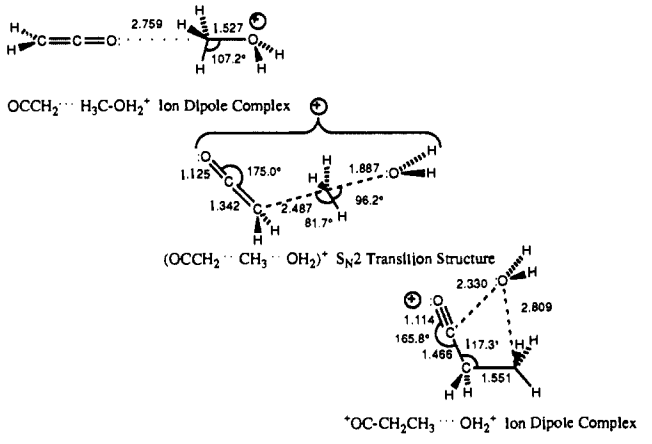

Figure 2. Partial geometries (distances in angstroms, angles in degrees) of ion–dipole complexes and the transition structure for S_N2 displacement of H_2O from $CH_3OH_2^+$ by $H_2C{=}C{=}O$. All these structures were calculated within C_s symmetry at the RHF level with basis sets as listed in Table VI. Selected geometrical variables shown were computed at the 6-31+G* level, except for those of the $(OC{-}CH_2CH_2\cdots OH_2)^+$ ion–dipole complex, which shows 3-21G values.

comparisons based on the gas-phase and calculated results.

Discussion

We begin by assuming that the initial C–C bond forming events in zeolite- and PPA-catalyzed conversions occur by related mechanisms. The observed absence of methane and the overall similarity of the product mixtures from the Mobil and Pearson processes are key in our choice of the Pearson reaction as a homogeneous model for the zeolite processes; H-ZSM-5 and PPA are almost unique among simple oxide catalysts in producing very little methane from the catalytic conversion of methanol. A second assumption is that free-radical processes have been ruled out.[11,24] The temperatures involved, at least in the Pearson reaction, do not approach those needed for bond homolysis, and it is unclear how the catalysts could significantly alter that situation. Any polar process that forms C–C bonds requires a carbon electrophile and a carbon nucleophile. Under the strongly acidic conditions of these reactions, there is no shortage of electrophilic "CH_3^+" fragments, in the form of protonated methanol or dimethyl ether, trimethyloxonium ions, or methylated-framework oxonium ions (Mobil process) or phosphates (Pearson reaction). On the other hand, it is difficult to envision a carbon nucleophile that would not be protonated in this setting. Thus, the crucial intermediate is that species in which carbon may act as a nucleophile to be methylated. In the Olah picture (Scheme I), the nucleophilic intermediate is the oxonium ylide, while the CO mechanism of Scheme III has ketene in the nucleophile's role.

In order to appreciate the proposed mechanism, it is useful to review certain key observations pertaining to the H-ZSM-5- and PPA-catalyzed MTG conversions. In the zeolite systems the following are observed: (1) Hydrocarbons appear in the product stream only after an induction period, regardless of whether methanol or dimethyl ether is used as the feed.[25] (2) Carbon monoxide is noted,[4] both in product streams and inside the zeolite cage; it is the first-formed intermediate seen in solid-phase ^{13}C NMR studies of the H-ZSM-5-catalyzed reaction,[3] though it is not always observed in such experiments.[15b] (3) Conditions producing ethylene generally yield some propene as well.[13c,14d,c] In our studies of the PPA system the following are observed: (4) No exchange is seen between acidic OH protons and methoxy CH protons. (5) Ethoxy groups are not observed in the ^1H NMR of reaction mixtures even under conditions that produce hydrocarbons. We note here, however, that Haw has found methyl ethyl ether in NMR studies of the Mobil process.[15a,b] (6) Observable quantities of gas-phase ethylene and dimethyl ether are present in the head space above the reaction mixtures.

Thermodynamic data from Figure 3 and Tables I–III also support the CO-catalyzed pathway. Here, each cycle of methylation and deprotonation is well within thermodynamic range.

(24) Hunter, R., Hutchings, G. J.; Pickl, W. *J. Chem. Soc., Chem. Commun.* **1987**, pp 843, 1369.

(25) (a) Ono, Y.; Mori, T. *J. Chem. Soc., Faraday Trans. I* **1981**, *77*, 2209. (b) Chen, N. Y., Reagen, W. J. *J. Catal.* **1979**, *56*, 268.

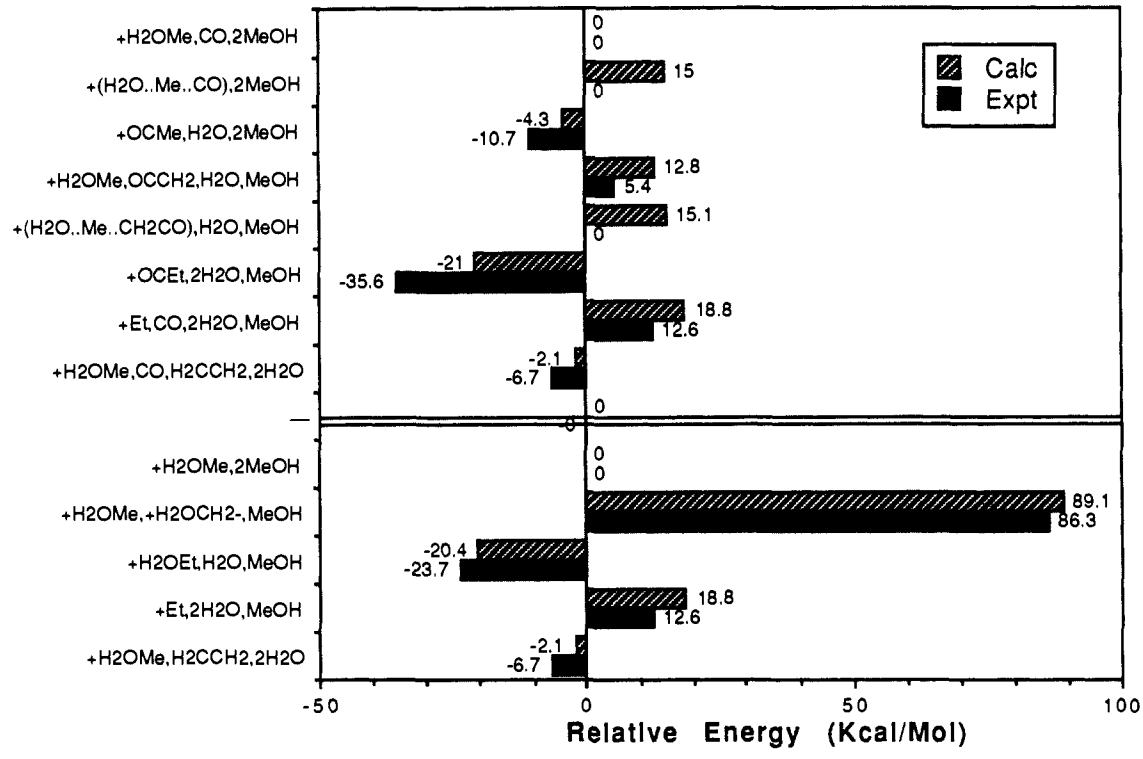

Figure 3. Reaction energy profile for the processes of Scheme III (upper) and Scheme II (lower), relative to starting materials at 0.0. Experimental (black) and theoretically calculated (hatched) energy values (in kilocalories per mole) are displayed for comparison to each other. Labels on the left signify the composition of the "reaction mixtures" at points along the reaction pathways. Naturally, for the TS structures (rows 2 and 5) there are no experimental energies, so these appear as 0.0. It should be noted that the largest excursion from the base line appears at the point of deprotonation of $CH_3OH_2^+$ to make $CH_2{}^-OH_2^+$, the oxonium ylide.

By contrast, the analogous set of calculations for the oxonium ylide series (Table IV, Figure 3) show that, barring special effects[24] due to the zeolite/PPA catalysts, the required deprotonations would be extremely unlikely at the temperatures employed or would require very strong (probably anionic) bases. This result is in accord with gas-phase observations that suggest that the strongest gas-phase bases are unable to deprotonate methylonium ions, even when assisted by added kinetic energy.[26] Thus, although Olah and co-workers have made a convincing case for the oxonium ylide scheme in strongly basic systems, we do not consider it to be a viable mechanism for conventional MTG processes.

Each step of the sequence in Scheme III is thermochemically accessible at the temperatures of these reactions. Given the known presence of all the required ingredients and the energetic accessibility of the CO catalytic cycle, it seems almost inevitable that such chemistry would occur to a substantial extent in these acidic systems. We now examine this new scheme step by step.

Alkylation of carbon monoxide by alkyl cations is a familiar reaction. Olah has recently reported electrophilic methylations of CO, likely via an S_N2 mechanism and leading ultimately to polyketene[27a] or acetic acid/esters,[27b] depending on conditions. Formation of carboxylic acids by reaction between secondary or tertiary carbocations and CO followed by H_2O quenching is a well-established reaction in organic synthesis.[27c] Gas-phase methyl cation transfers to and from N_2, isoelectronic to CO, are also common.[21b] Thermochemically, reaction of CO with protonated methanol as a methyl cation donor is a favorable process as shown in Table II. Although the proton affinity (PA) of H_2O is greater than that of CO, the corresponding methyl cation affinities (MCA's) are inverted, with CO binding CH_3^+ ~10 kcal/mol more tightly than does H_2O.[21]

In order to assess the *kinetic* accessibility of the methyl transfer from $CH_3OH_2^+$ to CO, we have run a series of ab initio calculations on this reaction. The energies and critical geometrical parameters of the separated species, the ion–molecule complexes, and the methyl-transfer transition structure are collected in Table V, while Figure 1 illustrates points on the hypothetical reaction potential energy surface. The calculated activation energy between ion–dipole complexes is 16.4 kcal/mol, and the reaction energy is −4.3 kcal/mol. These values are reasonable in light of the estimate by Bowers et al. that, for the reaction $CH_3OH + CH_3OH_2^+ \rightarrow (CH_3)_2OH^+ + H_2O$, the activation barrier is 1.05–1.2 eV (24–28 kcal/mol) and the reaction exothermicity is 0.6 eV (14 kcal/mol).[28] For comparison, we obtain an exothermicity of 14.8 kcal/mol (Table IV) from our calculations, while the experimental value (Table I) is 15.2 kcal/mol.

Solution studies of acylium cations under superacid or near-superacid conditions provide further evidence of the nucleophilic capabilities of ketene and its accessibility from the acetyl cation (or acylium ion, CH_3CO^+). When acylium ion is generated from the reaction of acetyl chloride with $AlCl_3$, substantial quantities of diacetylated species **12** are observed when the medium is insufficiently acidic.[29a] It is assumed that these products arise by deprotonation of acylium ion to make ketene, followed by acetylation to generate acetylacylium ion. Repetition of the process yields the observed diacetylated product **12**. The absence of the

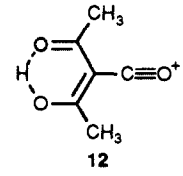

12

(26) Squires, R. Personal communication.

(27) (a) Olah, G. A.; Zadok, E.; Edler, R.; Adamson, D. H.; Kasha, W.; Prakash, G. K. S. *J. Am. Chem. Soc.* **1989**, *111*, 9123. (b) Bagno, A.; Bukala, J.; Olah, G. A. *J. Org. Chem.* **1990**, *55*, 4284. (c) Bahrmann, H. In *New Syntheses with Carbon Monoxide*; Falbe, J., Ed.; Reactivity and Structural Concepts in Chemistry Series 11; Springer-Verlag: Berlin, 1980; Chapter 5, p 372.

(28) Bass, L. M.; Cates, R. D.; Jarrold, M. F.; Kirschner, N. J.; Bowers, M. T. *J. Am. Chem. Soc.* **1983**, *105*, 7024.

(29) Olah, G. A.; Germain, A.; White, A. M. In *Carbonium Ions*; Olah, G. A., Schleyer, P. V. R., Eds.; Wiley Interscience: New York, 1976; Vol. 5, Chapter 35, pp 2084, 2115.

monoacetylated species is noteworthy here, in light of Mole's observation of propene production under all conditions that yield ethylene from CH_3OH/H-ZSM-5 reactions.[13c,14d,e] There are also a few examples[29b] of *alkylation* of ketenes in the literature, which, together with the above acylation reactions, provide reasonable precedents for the ketene methylation we propose here.

To learn more about the barriers and structures involved in the critical new C–C bond forming step, we have computationally examined the details of ketene alkylation by methyl cation transfer from $CH_3OH_2^+$ to ketene. The results of these calculations are presented in Table VI and Figure 2. As was found for the methylation of CO, the activation barrier for methylation (ca. 17 kcal/mol from the ion–dipole complex) is well within the thermally accessible range at the reaction temperatures. As mentioned above, literature examples of simple ketene alkylation are scarce, but electrophilic alkylation of analogous sp^2 carbon sites in olefins is quite familiar; indeed, it is the expected mechanism for zeolite-catalyzed olefin and aromatic alkylation processes.[30] In light of the very similar PA and MCA values between ketene and isobutene, the steric similarities between the sites to be alkylated, and the established capability of the latter olefin to be methylated, the analogous methylation of ketene seems entirely reasonable. Calculations at the 3-21G level (no vibrational corrections) support this notion, yielding an ion–molecule complex bound by 6.3 kcal/mol for isobutene (compare 11.7 for ketene) and a transition structure located 8 kcal/mol higher in energy than the separated fragments. Structurally, the ketene and isobutene methylation transition structures are also quite similar.

Gas-phase data and our calculations both suggest that deprotonation of acylium ion may be the most endothermic step in the overall reaction scheme. However, as described above, products have been observed from acylium ion equilibration with ketene under conditions more acidic and lower in temperature than MTG reactions.[29a] Thus, given the intermediacy of the acylium ion, ketene is clearly an accessible intermediate. We note here that all attempts to compute the barrier to proton transfer from H_3O^+ to ketene showed a monotonically exothermic process. No ketene–H_3O^+ ion–dipole intermediate could be located.

For comparison to the acylium ion/ketene system, we may ask how energetically accessible are the key oxonium ylide intermediates in Schemes I and II (see Figure 3). Our calculations suggest that the PA's of $CH_2{}^-OH_2^+$ and of $CH_2{}^-O^+(CH_3)_2$ are 266 and 281 kcal/mol, respectively, more than ~70 and ~80 kcal/mol, respectively, higher than the calculated 194 kcal/mol PA of ketene. A more accurate estimate of the PA of $CH_2{}^-OH_2^+$ is obtained by combining the high-level ab initio results[31] of Pople et al. with the experimentally known PA of methanol. According to these authors, the energy difference between CH_3OH and its isomeric structure $CH_2{}^-OH_2^+$ is 86.3 kcal/mol; adding this value to the 182 kcal/mol experimental PA of methanol yields a PA of 268 kcal/mol for $CH_2{}^-OH_2^+$, the simplest oxonium ylide. This number exceeds ketene's PA of 198 kcal/mol by a whopping 70 kcal/mol, supporting the results of our own calculations. Thus, deprotonation of the methyloxonium ions examined here is energetically out of reach in the absence of very strong bases. Unless the H-ZSM-5 or PPA catalysts can exert some unique acidifying influence on the methyloxonium ions in Scheme I and II, it is unclear how methyleneoxonium ylides could play a role in MTG reactions.

One apparently contradictory literature report must be addressed.[13c] We observe no hydrogen isotope exchange between acidic *H*O and methoxyl *H*CH_2O sites in the Pearson reaction at 200 °C. However, Mole's careful labeling studies do show such exchange occurring at 350 °C in the H-ZSM-5 system.[13c] At first glance this result might seem to be critical evidence for the methyleneoxonium ylide pathway or an indication that the overall reactions are unrelated. However, a preferable interpretation is that the methyl group transfer from CO *back* to ether, alcohol, or catalyst oxygen sites is accessible at the higher temperatures of the zeolite process. Examination of Table I shows that the experimental gas-phase MCA values for water (68 kcal/mol), methanol (83 kcal/mol), and dimethyl ether (~92 kcal/mol) bracket that of CO (78 kcal/mol), suggesting that methyl group transfer in either direction might occur. It is clear that the HCH_2CO^+ protons of acylium ions are easily exchanged. If the barriers to methyl back-transfer were just a bit higher than for deprotonation and methylation, the apparent exchange process might only "turn on" at higher temperatures. Furthermore, in the groundbreaking work of Chang and Silvestri, it was found that acetic acid reacts over H-ZSM-5 to give principally isobutene.[5a] Although the authors did not comment on this fact, if XYO^+CH_3 intermediates are critical in the Mobil process, the reverse methyl group transfer (or some brand new mechanism) needs to be invoked to gain access to methylating species and hence to the product spectrum seen.

After ketene methylation to **9**$^+$, S_N1 cleavage gives CO and ethyl cation, which easily loses a proton to the catalyst, yielding the observed ethylene. This cleavage may also be formulated as a concerted E2 elimination of the elements of HCO^+ to give protonated catalyst, ethylene, and CO directly. Alternatively, α-deprotonation gives methylketene **10**, which may be methylated a second time; subsequent loss of a proton and CO leads to propene. It is important to note (Table II) that as the extent of methylation increases, a sharp drop is seen in the strength of the R–CO^+ bond of acylium ions. Loss of CO from alkyl cations is simply the reverse of the olefin carboxylation reactions discussed previously and is well established for situations in which a secondary or tertiary alkyl cation will be left behind.[32] Thus, the second methylation yields an acylium cation **11**$^+$ that is rapidly cleaved, and the propene to ethene product ratio would actually be expected to drop as the temperature is increased, favoring cleavage of **9**$^+$ over deprotonation to **10**. At the elevated temperatures involved in MTG reactions, such a cleavage reaction should be facile; the analogous elimination of water from higher alcohols such as ethanol and 2-propanol occurs readily in these systems.[9,13c,15f]

Why has the CO-catalyzed mechanism not received attention earlier? Surely someone must have observed that addition of CO reduces or eliminates the induction period in MTG chemistry. Indeed, over 12 years ago, Derouane et al.[9] used NMR to study the effect on the Mobil process of added CO. Although the authors did not comment on it, the data displayed in their paper clearly show that in the absence of added CO no hydrocarbons were observed until the *second* spectrum was taken (ca. 8 min at 350 °C). When CO was added, these products appeared in the very first measurement (ca. 4 min) and increased linearly. Similarly, Hutchings et al.[12] studied the effect on the reaction of formic acid and formaldehyde additives, concluding that formic acid is relatively harmless and that formaldehyde deactivates the MTG catalyst rapidly. Unfortunately, the early phases of these reactions were not reported so that no conclusions can be reached about the effects of these additives on the induction period. We can only speculate about the mechanism of catalyst deactivation by formaldehyde; perhaps ketene may function like a Wittig reagent as follows:

$$H_2C{=}O + H_2C{=}C{=}O \rightarrow H_2C{=}CH_2 + O{=}C{=}O$$

This process would result in a net oxidation of CO to CO_2, removing it from the catalytic cycle and shutting down the reaction. Alternatively, formaldehyde may just facilitate coking and, hence, deactivation of the zeolites via some unspecified mechanism.

The details of the initial CO generation remain in question. In zeolites, the recent work of Klinowski and Anderson[3] has established it as the first-formed observable product, though Haw has questioned this result.[15b] The reaction conditions of the Mobil process are known to oxidize formaldehyde or its equivalents to produce CO.[5a,12] Thus, the CO presumably arises by oxidation

(30) (a) Oda, R., Muncimiya, S., Okano, M. *J. Org. Chem.* **1961**, *26*, 1341. (b) Hofmann, J. E., Schriesheim, A. In *Friedel-Craft and Related Reactions*; Olah, G. A., Ed.; Wiley Interscience: New York, 1976; Vol. 2, Chapter 19, pp 622, 623.

(31) Pople, J. A.; Ragavachari, K.; Frisch, M. J.; Binkley, J. S.; Schleyer, P. v. R. *J. Am. Chem. Soc.* **1983**, *105*, 6389.

(32) See ref 29, pp 2123 ff.

of methanol during the initial induction period, perhaps by protons or methyloxonium ions, which function as methyl cation equivalents; later, as olefins are generated, carbocations (from protonation of olefins) must become the hydride acceptors. This suggestion is consistent with the substantial fraction of fully saturated hydrocarbons produced by these reactions.[5] Such a product spectrum would obviously be impossible without a net source of hydrogen.

The CO-catalyzed mechanism explains the connection between propene and ethylene formation.[13c,14c,d] It further suggests several simple experimental tests, of which we have performed the first and most obvious. We have searched for exchange between the acidic *H*OX and the methoxy HCH_2OX protons and found none by running the Pearson reaction with CD_3OD. This observation suggests that for an oxonium methylide to be important in this reaction *it must be methylated at a much greater rate than it is reprotonated*. Since this process is kinetically unlikely in the unstructured PPA solution, we conclude from our experiments that the oxonium methylide mechanism is not operating in the 200 °C PPA-catalyzed transformation of methanol into hydrocarbons. We are currently conducting experiments to determine whether added CO or CO precursors significantly alter the timing and sequence of appearance of reaction products in the Pearson reaction. In addition, we are pursuing a collaborative effort to study the methylation reactions of CO and ketene by methyl cation donors such as protonated methanol in the gas phase.

Summary

We have proposed a new mechanism to account for the initial transformation of methanol into hydrocarbons by acidic oxide catalysts such as H-ZSM-5 or PPA. From their similarities in products, we infer that the Mobil process and the Pearson reaction occur by mechanisms that are essentially the same, in spite of the different compositions and structures of the catalysts. A familiar presence in the zeolite systems, CO is now seen as the active catalyst, at least in the reaction's early phases. H-ZSM-5 or PPA are relegated to the simple role of medium to strong Brönsted acids, which promote dehydration, are weakly able to oxidize methanol to CO in the initial period, and retain CO in the reacting medium. Our results for the Pearson reaction support this picture, principally by casting doubt on the oxonium ylide pathway. On thermochemical grounds and by the absence of observable OH/CH exchange in the methoxyl groups derived from methanol, the intermediacy of oxonium methylides in these MTG reactions seems highly unlikely. The story is less exciting without the relatively exotic oxonium ylides. It is more thermochemically reasonable, however, and it reaffirms the dominance of the carbonyl group in organic chemistry. In place of framework or phosphate oxygen and oxonium methylides, carbon monoxide and ketene are seen as the catalytic activating group and nucleophilic carbon species, respectively. By revealing the central role of CO, a gaseous byproduct, this new mechanistic scheme introduces a fresh paradigm for the design of catalysts and control of reactions.

Acknowledgment. Professor Donald Pearson has been outstandingly helpful in excavating and sharing his original PPA results; we are most grateful for his encouragement and wisdom. J.E.J. thanks the Camille and Henry Dreyfus foundation for a Distinguished Young Faculty award and Michigan State University for generous startup support. Professors G. A. Olah, J. F. Haw, and J. F. Liebman offered useful data, references, and suggestions; Dr. Evelyn Jackson assisted with our early multinuclear NMR work; Professor Michael Rathke contributed insights on phosphorus chemistry; and an enthusiastic freshman, Mike Vethacke, tested the earlier experimental designs that led to our decision to examine the Pearson reaction in situ by NMR.

Gas-Phase Proton Affinity of Deoxyribonucleosides and Related Nucleobases by Fast Atom Bombardment Tandem Mass Spectrometry

Francesco Greco, Angelo Liguori, Giovanni Sindona,* and Nicola Uccella

Contribution from the Dipartimento di Chimica, Università della Calabria, I-87030 Arcavacata di Rende, Cosenza, Italy. *Received August 23, 1989. Revised Manuscript Received July 23, 1990*

Abstract: The proton affinities (PA) of the deoxynucleosides and nucleobases present in DNA's have been determined from the kinetics of the gas-phase unimolecular dissociations of their proton-bound hetero-complexes with amines of known PA. The clusters have been formed by fast-atom-bombardment mass spectrometry from different matrices, whose effect has been evaluated. The experimentally determined order dG > dA ≅ dC ≫ dT differs from that of the corresponding pyrimidine and purine bases, Gua > Cyt > Ade ≫ Thy, and from that of the same nucleosides in aqueous solutions.

Introduction

Acid–base equilibria involving nucleic acid components have been widely investigated in polar and apolar solvents by spectroscopic means.[1] The determination of the pK_a values and of the protonation sites of nucleobases and nucleosides contributed to the understanding of the chemical processes undergone by DNA molecules in the condensed phase. The availability of desorption ionization (DI) methods in mass spectrometry (MS)[2,3] has favored a rapid growth of gas-phase investigations in the field of nucleic acid chemistry.[4-8] Moreover, the properties of the DI method known as fast-atom-bombardment (FAB)[9] have opened new

(1) Saenger, W. *Principles of Nucleic Acid Structure*; Springer-Verlag: New York, 1984; pp 105-115.
(2) Fenselau, C.; Cotter, R. J. *Chem. Rev.* **1987**, *87*, 501-512.
(3) Pachuta, S. J.; Cooks, R. G. *Chem. Rev.* **1987**, *87*, 647-669.
(4) Panico, M.; Sindona, G.; Uccella, N. *J. Am. Chem. Soc.* **1983**, *105*, 5607.
(5) Tomer, K. B.; Gross, M. L.; Deinzer, M. L. *Anal. Chem.* **1986**, *58*, 2527.
(6) Rogan, E. G.; Cavalieri, E. L.; Tibbels, S. R.; Cremonesi, P.; Warner, C. D.; Nagel, D. L.; Tomer, K. B.; Cerny, R. N.; Gross, M. L. *J. Am. Chem. Soc.* **1988**, *110*, 4023.
(7) Liguori, A.; Sindona, G.; Uccella, N. *Biomed. Environ. Mass Spectrom.* **1988**, *16*, 451.
(8) Liguori, A.; Sindona, G.; Uccella, N. *J. Chem. Soc., Perkin Trans. 2* **1988**, 1661.

0002-7863/90/1512-9092$02.50/0